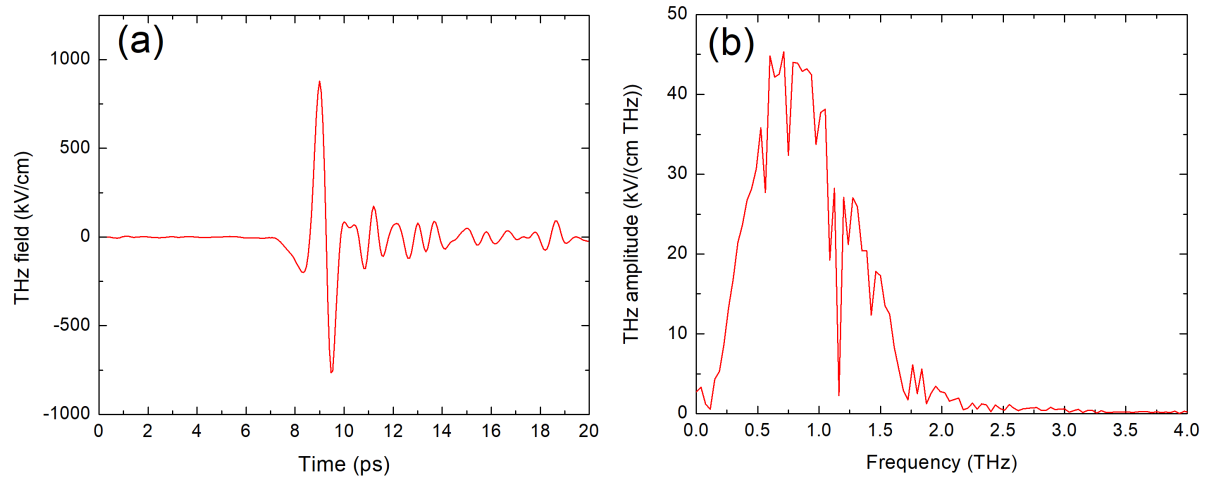
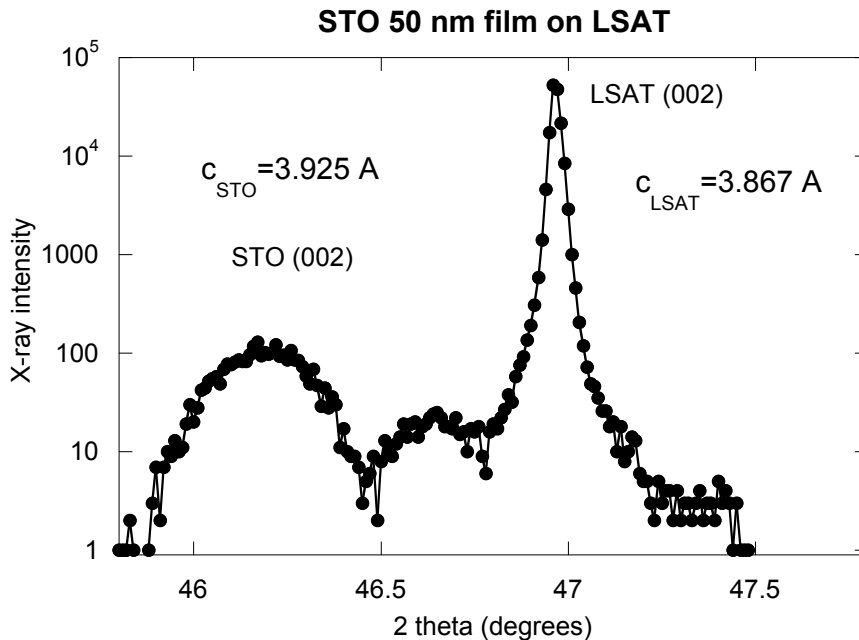


# Supplementary material

Kozina et al, "Terahertz-Driven Phonon Upconversion in  $\text{SrTiO}_3$ "



**Figure S1 Terahertz pump waveform:** **a** Electro-optic sampling signal of terahertz (THz) pump at sample location measured in-situ by electro-optic sampling in a 50  $\mu\text{m}$  thick (110) GaP crystal. **b** Magnitude of frequency spectrum of the THz waveform in **a** calculated by Fast Fourier Transform. The intensity was adjusted with wiregrid polarizers (Infraspecs P01) without changing the THz waveform.



**Figure S2: Two-Theta scan of sample before annealing.** Static x-ray diffraction pattern along sample normal. The low-angle peak corresponds to the STO film and the sharp peak at higher angle is the LSAT substrate. We observe clear splitting along the cross-plane direction between the substrate and the film. These measurements were taken before the sample was annealed.

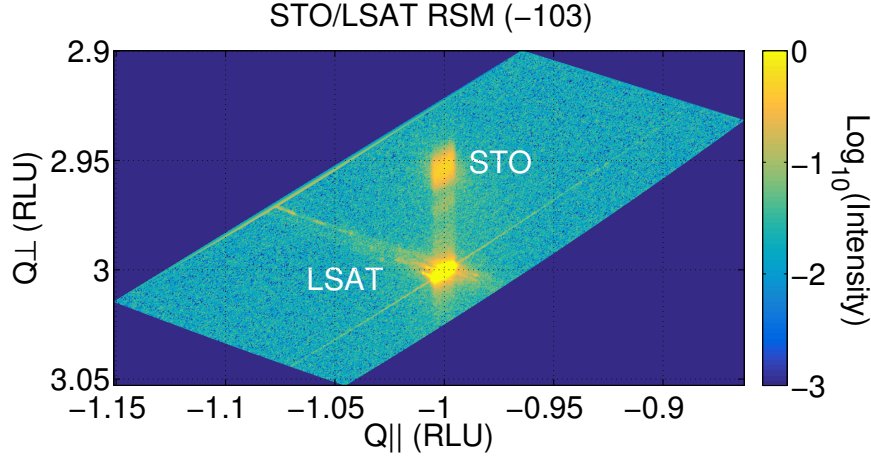


**Figure S3: Reciprocal space map of the sample before annealing.** Static reciprocal space map collected on a similar sample prior to annealing about the  $(-1\ 0\ 3)$  reciprocal lattice point using a  $\text{Cu } \alpha$  source. The separation between the film and substrate peaks along the cross-plane direction shows there is a difference in lattice parameter, whereas there is clear indication that in-plane the film and substrate are lattice matched to the LSAT unit cell.

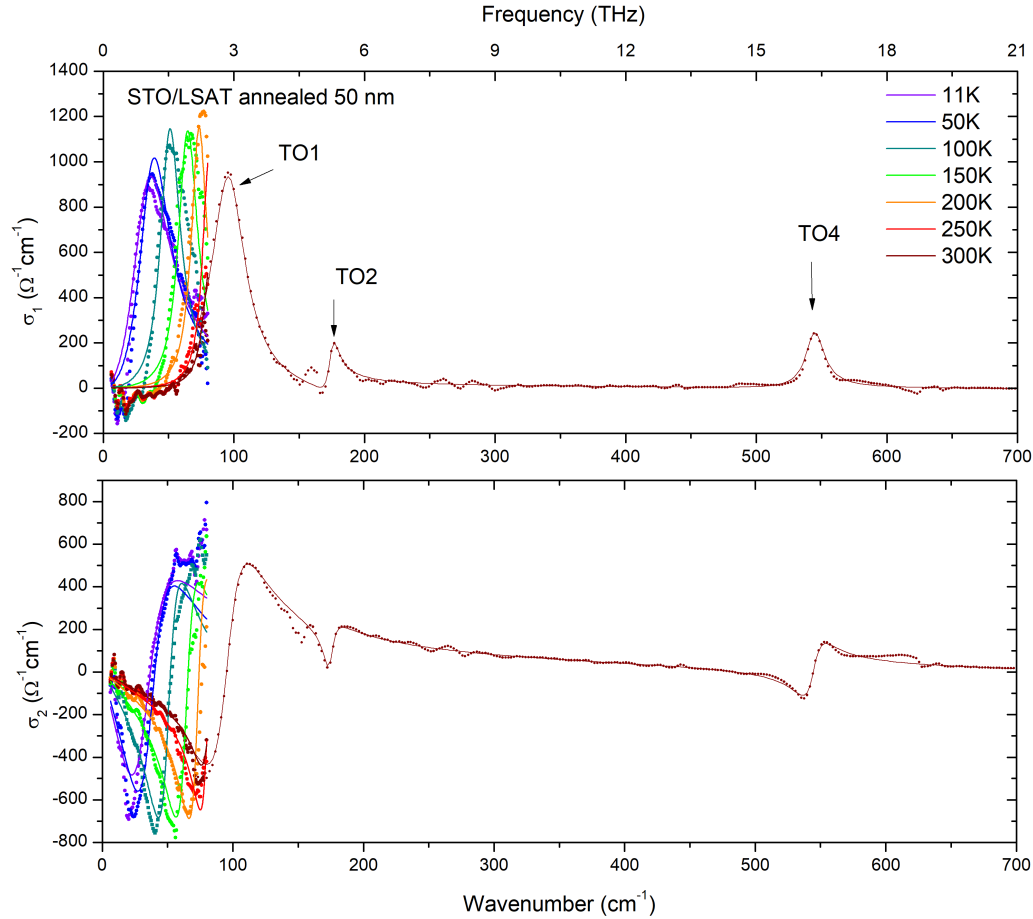


**Figure S4: Optical conductivity of the annealed sample.** We show additional ellipsometry measurements on our sample incorporating extra temperature points at low and high temperature. The extended frequency range at 300K shows the  $\text{TO}_2$  and  $\text{TO}_4$  phonon modes. Data from Fig. 3a are also included for comparison.

	Sr	Ti	Oxy	Ozx	Oyz
X	0	0.5	0.5	0.5	0
Y	0	0.5	0.5	0	0.5
Z	0.00987045	0.51190984	0.9970011	0.4956093	0.4956093

**Table S1 Unit Cell Relative Coordinates from DFT.** Lattice is tetragonal with  $a_0 = 3.89000 \text{ \AA}$  and  $c_0 = 3.91043 \text{ \AA}$ .

	Sr	Ti	Oxy	Ozx	Oyz
X	0.02963898	0.04544241	-0.08189972	-0.09030182	-0.07348941
Y	-0.02957567	-0.04530107	0.08204853	0.07359076	0.09041028
Z	0	0	0	0	0

**Table S2 Eigenvector for  $Q_1$  mode.** Eigenvector calculated with  $E_{\text{THz}}$  parallel to  $(X, -Y, 0)$ . The units of the eigenvector are  $\text{\AA}^* \text{AMU}^{1/2}$ . The eigenvector is normalized so that  $\sum \xi_{ijk}^2 m_{jk} = 1$ . Here  $\xi_{ijk}$  and  $m_{jk}$  are the eigenvector and ion mass in AMU, and the indices  $i, j, k$  label the eigenvector mode, ion, and coordinate direction.

	Sr	Ti	Oxy	Ozx	Oyz
X	-0.04831474	0.07770832	0.01575631	0.00874036	0.00874793
Y	0.04829799	-0.07773579	-0.01568512	-0.00870886	-0.00868356
Z	0	0	0	0	0

**Table S3 Eigenvector for  $Q_2$  mode.** Eigenvector calculated with  $E_{\text{THz}}$  parallel to  $(X, -Y, 0)$ . The units of the eigenvector are  $\text{\AA}^* \text{AMU}^{1/2}$ . The eigenvector is normalized so that  $\sum \xi_{ijk}^2 m_{jk} = 1$ . Here  $\xi_{ijk}$  and  $m_{jk}$  are the eigenvector and ion mass in AMU, and the indices  $i, j, k$  label the eigenvector mode, ion, and coordinate direction.

$\omega_1/(2\pi)$	<b>1.669 THz</b>	$\kappa_1$	$8900 \text{ THz}^2 \text{\AA}^{-2} \text{AMU}^{-1}$	$\chi$	$4000 \text{ THz}^2 \text{\AA}^{-2} \text{AMU}^{-1}$
$\omega_2/(2\pi)$	<b>5.186 THz</b>	$\kappa_2$	<b>1066 THz<sup>2</sup>Å<sup>-2</sup>AMU<sup>-1</sup></b>	$\psi_{12}$	$-4000 \text{ THz}^2 \text{\AA}^{-2} \text{AMU}^{-1}$
$\gamma_1/(2\pi)$	<b>0.900 THz</b>	$Z_1^*$	<b>2.6 e<sup>-</sup>AMU<sup>-1/2</sup></b>	$\psi_{21}$	<b>-841 THz<sup>2</sup>Å<sup>-2</sup>AMU<sup>-1</sup></b>
$\gamma_2/(2\pi)$	0.150 THz	$Z_2^*$	<b>0.2 e<sup>-</sup>AMU<sup>-1/2</sup></b>	$\beta$	0.215

**Table S4 Model parameters.** Values in bold are unmodified from DFT calculations at 0 K. Values in red were extracted from spectroscopy and literature. Parameters  $\kappa_1$ ,  $\psi_{12}$ , and  $\chi$  were initially established by DFT and then tuned to best fit the experimental data. The parameter  $\beta$  was informed by calculations for the expected field screening inside the STO film on the LSAT substrate but was fine-tuned to best fit the experimental data. The linewidth  $\gamma_2$  was estimated from the trXRD data in the frequency domain.

## Comments on Mode Symmetry in STO Film

In bulk STO, there are four sets of optical phonons, with symmetries (in order of increasing frequency)  $T_{1u}$ ,  $T_{1u}$ ,  $T_{2u}$ , and  $T_{1u}$  [S1]. The three  $T_{1u}$  modes are all IR active and in addition possess LO/TO splitting. The  $T_{2u}$  mode is known as “silent” because it lacks both IR and Raman activity [S2]. This mode lacks TO/LO splitting. The mode frequencies at 85K are presented in Table S5 and labeled according to [S3].

Mode	Frequency (cm <sup>-1</sup> )	Frequency (THz)
TO <sub>1</sub> (soft)	31	0.93
LO <sub>1</sub>	170.6	5.114
TO <sub>2</sub>	172.5	5.171
T <sub>2u</sub> (TO <sub>3</sub> , LO <sub>2</sub> ) (silent)	265	7.94
LO <sub>3</sub>	469.5	14.08
TO <sub>4</sub>	544	16.3
LO <sub>4</sub>	801	24.0

*Table S5 Bulk STO Mode Frequencies at 85 K. Values are extracted from Barker [S3].*

In our film, however, the substrate is compressive and makes the STO film slightly tetragonal (see static x-ray characterization in Figure S2). This alters the symmetries of the four modes according to the rules:  $T_{1u} \rightarrow A_1 + E$ ,  $T_{2u} \rightarrow B_1 + E$ . The  $A_1$  and  $B_1$  modes consist of displacements along the cross-plane component, while the  $E$  modes consist of displacements in-plane. This splitting should also adjust the frequencies of the modes.

The incident THz field resonantly couples to a near-zone center transverse optical mode (the soft mode) with displacement along the THz polarization direction,  $[1 -1 0]$ , and with wavevector parallel to the THz wavevector (cross-plane direction). Thus the excited soft mode has displacement vector along  $[1, -1, 0]$  and wavevector along  $[0 0 1]$ , and has symmetry  $E$ . In addition to observing this feature in our trXRD signal, we also detect oscillations at 5.15 THz and 7.6 THz, close in frequency to the LO<sub>1</sub>/TO<sub>2</sub> and T<sub>2u</sub> (silent) modes in bulk STO.

We suspect that the strongest coupling between the soft mode and other phonon modes will occur for modes with the same symmetry and with the same wavevector and displacement directions, hence we attribute the oscillatory components at 5.15 and 7.6 THz to transverse optical phonons with displacements along  $[1 -1 0]$  and wavevectors along  $[0 0 1]$ , also of symmetry  $E$ . We then label these three coupled modes as TO<sub>1</sub>, TO<sub>2</sub>, and TO<sub>3</sub> in order of increasing frequency. From our numerical calculations of the nonlinear phonon coupling terms, we find that  $T_{1u}(\text{soft}) \rightarrow T_{2u}(\text{silent})$  coupling while possible is much weaker than  $E(\text{soft}) \rightarrow E(\text{silent})$ .

Our x-ray measurements, however, are unable to detect whether the atomic displacements we observe are in-plane or cross-plane, because we measure an x-ray diffraction peak that is nearly equally sensitive to in-plane and cross-plane motion,  $hkl = (2 -2 3)$ . We cannot rule out, therefore, by our experimental measurement that the modes to which the soft mode couples are not longitudinal.

References:

S1. Cowley, R. A. Lattice Dynamics and Phase Transitions of Strontium Titanate. *Phys. Rev.* **134**, A981–A997 (1964).

S2. Denisov, V. N., Mavrin, B. N., Podobedov, V. B. & Scott, J. F. Hyper-Raman Spectra and Frequency Dependence of Soft Mode Damping in SrTiO<sub>3</sub>. *J. Raman Spectrosc.* **14**, 276–283 (1983).

S3. Barker, A. S. Temperature dependence of the transverse and longitudinal optic mode frequencies and charges in SrTiO<sub>3</sub> and BaTiO<sub>3</sub>. *Phys. Rev.* **145**, 391–399 (1966).